



HAL
open science

New feature of DARWIN/PEPIN2 inventory code: Propagation of nuclear data uncertainties to decay heat and nuclide density

A. Tsilanizara, T.D. Huynh

► To cite this version:

A. Tsilanizara, T.D. Huynh. New feature of DARWIN/PEPIN2 inventory code: Propagation of nuclear data uncertainties to decay heat and nuclide density. *Annals of Nuclear Energy*, 2021, 164, pp.108579. 10.1016/j.anucene.2021.108579 . cea-04490573

HAL Id: cea-04490573

<https://cea.hal.science/cea-04490573>

Submitted on 22 Jul 2024

HAL is a multi-disciplinary open access archive for the deposit and dissemination of scientific research documents, whether they are published or not. The documents may come from teaching and research institutions in France or abroad, or from public or private research centers.

L'archive ouverte pluridisciplinaire **HAL**, est destinée au dépôt et à la diffusion de documents scientifiques de niveau recherche, publiés ou non, émanant des établissements d'enseignement et de recherche français ou étrangers, des laboratoires publics ou privés.



Distributed under a Creative Commons Attribution - NonCommercial 4.0 International License

New feature of DARWIN/PEPIN2 inventory code : Propagation of nuclear data uncertainties to decay heat and nuclide density

A. Tsilanizara^{a,*}, T.D. Huynh^a

^a*DES-Service d'études des réacteurs et de mathématiques appliquées (SERMA), CEA, Université Paris-Saclay, F-91191, Gif-sur-Yvette, France*

Abstract

DARWIN/PEPIN2 is a French inventory code that has been developed at CEA since the mid-1990s for fuel fission reactor, material neutron activation and material radioactive decay calculations. It takes into account both R&D and industrial application requirements. Today, DARWIN/PEPIN2.4.x is the last major release and deals with nuclear data uncertainties propagation to some quantities of interest outputs as atom density, activity and decay heat. The purpose of this paper is to outline this last capability. Methodology approach, calculation hypotheses and nuclear data uncertainty used are discussed as well as the computational implementation. The last part of this paper shows two illustrative uncertainty calculations related to fission pulse and PWR-UO₂ fuel depletion configurations.

Keywords: DARWIN/PEPIN2, Sensitivity, Uncertainty, Decay Heat, Decay Data, Cross Section, COMAC, JEFF-3.1.1, ENDF/B-VII.1, JENDL/FPY-2011, JENDL/DDF-2015.

1. Introduction

DARWIN/PEPIN2 [1] is an inventory code developed at CEA since the mid-1990s for radioactivity related studies in various application fields (nuclear fuel cycle, dismantling, ...). It solves simultaneous ordinary differential equations describing the transmutation, the growth and the decay of the nuclide densities, and performs an accurate depletion calculation with fine description of the irradiation history and the isotopic chain. From nuclide concentration results, a large range of physical quantities can be calculated like nuclide mass, radioactivity, decay heat, decays α , β , γ emission, neutron source from spontaneous fission, delayed neutron and (α ,n) reaction. These physical quantities (Quantity Outputs of Interest or QOI) can be computed at any cooling times. QOI assessments with DARWIN/PEPIN2 have reached a great reliability as a consequence of its use feedback over two decades in both industrial applications and R&D [7] [9]. However it is crucial to control the reliability of the calculation results with a realistic estimation of the associated uncertainties due to uncertainties in the input nuclear data among other.

*Corresponding author. Tel : +33 1 69 08 65 37

Email addresses: aime.tsilanizara@cea.fr (A. Tsilanizara), tan-dat.huynh@cea.fr (T.D. Huynh)

Over the past years, DARWIN/PEPIN2 developments address on this task and lead nowadays to DARWIN/PEPIN2.4.x releases. Section 2 gives an overview of DARWIN/PEPIN2 code. Nuclear data and the available associated uncertainties are presented in section 3. Section 4 describes the methodology approach and its implementation in DARWIN/PEPIN2 code to propagate the nuclear data uncertainties through the entire calculation scheme. Decay heat and atom density uncertainties results, corresponding to some applications (Fission pulse, PWR fuel cell), are discussed in section 5. Conclusions are given in section 6.

2. Overview of DARWIN/PEPIN2 code

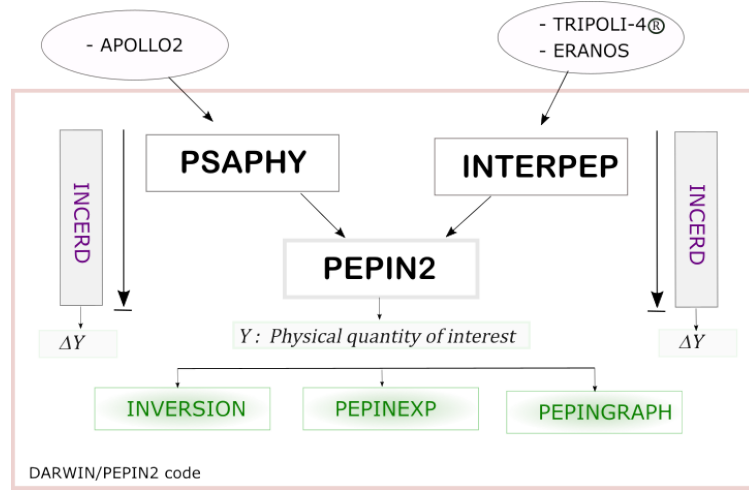


Figure 1: Modular structure of DARWIN/PEPIN2 code

As shown in figure 1, DARWIN/PEPIN2 code is organized in a modular structure. Each module performs a specific task which can be categorized as interface component with upstream transport code, Bateman equation solver component (PEPIN2), results post-treatment component. DARWIN/PEPIN2 has four main operating modes to assess the time dependant expected physical quantities, and one operating mode to deal with nuclear data uncertainties propagation to physical output quantities. These main calculation modes are :

a) Nuclear reactor fuel depletion with multi-step irradiation.

In this mode, the multi-group distribution of neutron fluxes and the self-shielded reaction cross-sections are provided by APOLLO2 [14], a CEA two-dimensional multi-group lattice spectral code. Additional multi-group cross-sections come from a GENDF (Group-wise ENDF) formatted library. The main physical quantity, the atom density $N_i(t)$ of different nuclide i in a homogenized fissile material region comes from the resolution of the following generalized Bateman equation using the quasi-static approximation :

$$\frac{dN_i(t)}{dt} = \sum_{k=1}^{N_f} \gamma_{k,i} \tau_k^f N_k(t) + \sum_{j \neq i} (b_{j,i} \lambda_j + \tau_{j,i}^r) N_j(t) - (\lambda_i + \tau_i) N_i(t) \quad (1)$$

where :

- N_f is the total number of fissile systems
- $\gamma_{k,i}$ is the fission yield of fissile nuclide k generating the fission product i
- τ_k^f is the fission rate of fissile nuclide k
- λ_i is the decay constant of nuclide i
- b_i is the decay branching rate of nuclide i
- $b_{j,i}\lambda_j$ is the decay rate of nuclide j to nuclide i
- $\tau_{j,i}^r$ is the neutronic transmutation rate of nuclide j to nuclide i by neutronic reaction r
- τ_i is the total disappearance rate of nuclide i by its neutronic transmutations

From the multi-group self-shielded cross sections and neutron spectra stored in so-called APOLLO2/SAPHYB file, PSAPHY module collapses the reaction rate data into one group structure or two groups structure in the case of fission reaction rate, in compliance with the irradiation time, for use in the PEPIN2 module to perform the inventory calculations.

b) Neutronic activation of a material structure with multi-step irradiation.

Unlike the previous mode, self-shielded cross sections are not required. As well, the first summation quantity appearing in the right side of equation (1) disappears as a result of the lack of fissile material. Activation cross-sections are fully provided in multi-group structure by GENDF library. Multigroup neutron fluxes for each irradiation step are earlier stored in open ascii format file which can be established from transport code outputs as TRIPOLI-4® [2], MCNP [4] or any other neutron transport codes. Instead of PSAPHY, INTERPEP module is used to collapse multi-group reaction rates into one group structure.

c) Neutronic activation of a material structure with successive irradiation pulses followed by cooling period.

This operating mode is characterized by very short irradiation pulses at high repetition rates during which radioactive decay process is neglected (pulse duration is assumed to be negligible compared to period between two successive pulses). The total fluence of the material during each pulse is expected as input of the INTERPEP module instead of neutron spectra. According to the use of total fluence, the simplified equation below is solved by PEPIN2 module in place of (1) :

$$\frac{dN_i(t)}{dt} = \sum_{l \neq i} \sigma_{il}^r S_0 E(t) N_l(t) + \sum_{j \neq i} \sigma_{ij} S_0 E(t) N_j(t) - \sigma_i S_0 E(t) N_i(t) \quad (2)$$

where S_0 is the total number of neutrons emitted during the k^{th} pulse operation and

$$E(t) = \begin{cases} \frac{1}{\epsilon} & \text{if } t_k \leq t \leq t_k + \epsilon \\ 0. & \text{otherwise} \end{cases}$$

d) **Cooling of initial radioactive material.**

This operating mode deals with the radioactive decay calculation of initial radioactive composition according to given cooling times.

e) **Sensitivity and uncertainty quantification.**

A fifth operating mode can be performed with the latest implemented module, the IncerD module. It addresses to the supervision of parallel calculations (figure 2) in the context of nuclear data uncertainties propagation to the physical QOI over the four previous operating modes. Section 4 exposes the implemented uncertainty calculation method. This supervision task is summarized by the figure 2. It involves of :

- the creation of input data files which provide the perturbation value of each perturbed parameter taken as one standard deviation (1σ) of the nominal value ;
- the launch of n parallel calculations, each calculation deals with one nominal computation and a set of perturbed computations. A perturbed computation is a calculation in which only one input uncertain parameter is perturbed. For the physical QOI, sensitivity coefficients to each perturbed input parameter is computed by finite difference between the nominal and perturbed calculations ;
- the collection of the computed sensitivity coefficients by all processors and their implementation in a matrix organization according to covariance data ;
- the computation of the first order formula propagation uncertainty given by the relation (4) in section 4.

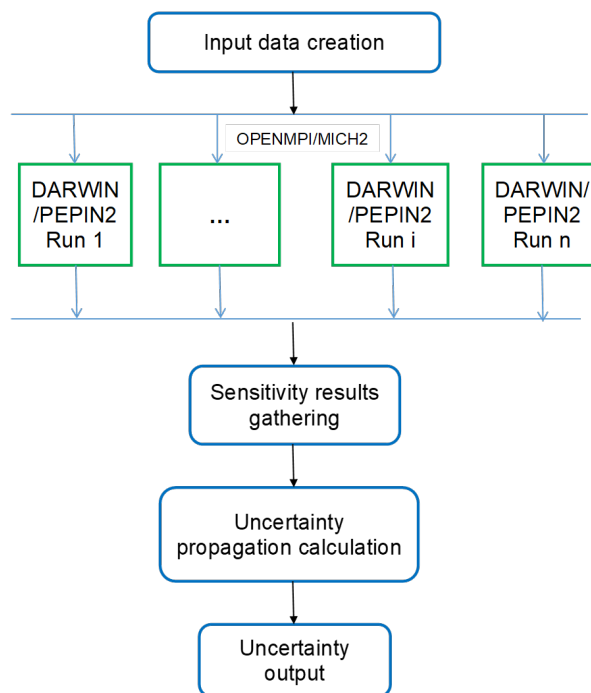


Figure 2: Diagram of uncertainty calculation with DARWIN/PEPIN2 using IncerD supervisor module.

From any DARWIN/PEPIN2 operating mode outputs, a following post-treatment modules can be implemented :

- INVERSION is dedicated to dominant pathways extraction for any nuclide of interest ;
- PEPINEXP deals with a set of functionalities which are :
 - saving outputs (activity, decay heat) in a Comma Separated Values format together with some decay data (period, decay energy) ;
 - saving outputs in specific format expected by PEPINGRAPH module, for graphical visualisation goal.
- PEPINGRAPH is based on ROOT library prerequisite developed by CERN [15]. It performs some graphical plots as :
 - the change over time of QOIs ;
 - the energy distribution of radiation source (α , β , γ , neutron) at a fixed cooling time.

3. Nuclear data uncertainties involved in decay heat uncertainty quantification

The energy released in irradiated nuclear fuel after reactor shutdown is called decay heat. This energy results from the activity of radionuclide (fission products and actinides) formed during the irradiation of nuclear fuel. $DH(t_c)$, the decay heat at the cooling time t_c , is calculated by the summation method given by the following equation :

$$DH(t_c) = \sum_{i=1}^n \lambda_i N_i(t_c) E_{avg,i} \quad (3)$$

where the atom density $N_i(t_c)$ is determined by solving the Bateman equations (1).

The decay heat is function of many physical parameters such as the decay constant (λ) and the total average energy (E_{avg}) released by decay of radionuclide. The radionuclide i , whose density is N_i , can be formed by many ways such as : decay of other radionuclide, fission of fissile nuclide, neutronic reactions, etc. . . Therefore, decay heat determination depends on additional parameters such as decay branching ratio (b_λ), fission yield (γ), neutronic reaction cross section (σ) and branching ratio of neutronic reactions (b_{xs}).

Uncertainty values of decay constants, decay branching ratios, average energies released by radioactive decay process, independent fission yields, are supplied by international nuclear evaluations : JEFF-3.1.1 [3] (3626 radionuclides and 39 fissioning systems), ENDF/B-VII.1 [5] (3576 radionuclides and 61 fissioning systems) and JENDL/DDF-2015 [10] (2993 radionuclides and 60 fissioning systems). DARWIN/PEPIN2 code uses mainly data from JEFF-3.1.1 libraries which provide about 40000 uncertain parameters (1554 for total average decay energy, 3205 for decay constant, 506 for decay branching ratio and over 32750 for fission yield of all fissioning systems). Table 1 gives the number of physical parameters with non-zero uncertainty value, for various libraries.

Table 1: Number of parameters with non-zero uncertainty value in various libraries

Parameter type	JEFF-3.1.1	ENDF/B-VII.1	JENDL/DDF-2015 & JENDL/FPY-2011
Total number of uncertain parameters	32751	41963	43827
²³⁵ U(T) ¹ Fission yield	918	998	1067
Decay Constant	3205	3270	2572
Decay branching ratio	506	988	1737
Decay total energy	1554	1718	2379

We emphasize the lack of correlation or covariance data in these libraries. Indeed, only uncertainty values are available. The obvious physical correlation between some parameters have led us to adopt some assumptions discussed in the following section.

4. Uncertainty quantification method

Uncertainty quantification with DARWIN/PEPIN2 code deals with two most important QOIs : total decay heat ($DH(t_c)$) and nuclide density ($N_i(t_c)$) at any cooling time t_c , where subscript i refers nuclide i . The deterministic methodology used to propagate input nuclear data uncertainties to these QOIs is based on the first order Taylor development in the vicinity of input parameter nominal value [21] [22], and relies on the hypothesis of linearity of the outputs vis-à-vis the introduced perturbation. We take one standard deviation of the nominal value (1σ) for each perturbation. This choice was validated by comparison with probabilistic uncertainty propagation approach which is based on stochastic sampling method and doesn't rely on linearity hypothesis, as seen in previous publications [24] and [25]. Adopting the following formal notations:

- $\vec{X} = \{\lambda_i, b_i, E_{avg,i}, \gamma_i, \tau_i\}$ for input parameters, ($i = 1, \dots, n$)
- $\vec{Y} = \{DH(t_c), N_i(t_c)\}$ for physical output quantities with $Y = DH(t_c)$ or $Y = N_i(t_c)$

Y uncertainty is given by the following formula :

$$Cov(Y) = S_{Y/X} Cov(X) S_{Y/X}^t \quad (4)$$

where $Cov(Y)$, $Cov(X)$ are respectively the variance-covariance matrix of response Y (total decay heat or nuclide density) and input parameter X (decay constants, decay branching ratios, mean decay energies, fission yields, ...). $S_{Y/X}$, $S_{Y/X}^t$ are respectively the sensitivity vector due to input parameter X and its transpose. The sensitivity coefficients, which are the $S_{Y/X}$ components, are built for each input parameter by direct perturbation calculations. That means:

$$S_{Y/X} = \frac{Y(X + \delta X) - Y(X)}{Y(X)} \bigg/ \frac{\delta X}{X} \quad (5)$$

With this additionnal capability, if we denote X by $M(X)$, the expected value of X , and Y by $M(Y)$, the expected value of Y , the new code inputs are $\{M(X), Cov(X)\}$ and the outputs are

$\{M(Y), Cov(Y)\}$. Nevertheless from $Cov(Y)$, the diagonal term, i.e, $Var(Y)$ is extracted and then the final results considered are $\{M(Y), \sqrt{Var(Y)}\}$, respectively the expected value of Y and the one standard deviation of this expected value. In practice, while diagonal terms of $Cov(X)$ are available from international nuclear evaluations, this is not the case for the off-diagonal terms. The exception concerns cross sections for which we use covariance data from the COMAC-V2.0 database [12]. In this database, correlation between partial cross sections for one given nuclide are provided in 26 and 33 energy groups mesh.

Due to lacks of covariance data provided by evaluations and accessible physical models that enable to assess them, both decay constants and mean energies are assumed to be uncorrelated, the off-diagonal terms of their respective covariance matrix are set equal to zero. For decay branching ratios or fission yields, these off-diagonal terms are derived from physical constraints between them as we outlines in the following paragraphs. A specific implementation was made in the IncerD module to build these covariance data.

4.1. Decay branching ratios

The decay branching ratio is defined as the ratio of the partial decay constant to the overall decay constant, multiple ($m > 1$) decay branching ratios attached to one radioactive nuclide must satisfy the following relationship :

$$\sum_{j=1}^m b_{i,j} = 1 \quad (6)$$

i.e, the sum of all decay branching ratios j from the same radionuclide i is equal to 1.

The variance of the previous sum can be expressed by :

$$Var\left(\sum_{j=1}^m b_{i,j}\right) = 0 \quad (7)$$

Then, the correlation coefficient $r_{i,j,k}$ between two decay branching ratios j and k from the same radionuclide i would be given by :

$$r_{i,j,k} = \frac{-\sum_{j=1}^m Var(b_{i,j})}{2 \sum_{j=1}^{m-1} \sum_{k=j+1}^m \sqrt{Var(b_{i,j})Var(b_{i,k})}} \quad (8)$$

Rigorously, for $m = 2$, variance values of both decay branching ratios have to be identical and this is generally the case that one encounters in data libraries provided by international evaluations. Nevertheless, to address with the exception of a few inconsistencies, the following consideration is made and generalized to $m = 3$ (in practice $m \leq 3$) :

Noting $\xi_{max} \neq 0$ the variance value of the dominant branching ratios attached to nuclide i , for each k where $Var(b_{i,k}) \neq \xi_{max}$, if $b_{i,k} - \sqrt{\xi_{max}} \geq 0$, $Var(b_{i,k})$ is set equal to ξ_{max} . Without this consideration, some data inconsistency would lead to calculated correlation coefficient value to be outside the $[-1, +1]$, which makes no sense at all.

4.2. Fission yields

To build fission yields covariance matrix, two options are available. First, we consider binary fission yields for which we have the following relationship :

$$\sum_{k=1}^{N_{FP}} \gamma_{i,k} = 2 \quad (9)$$

where N_{FP} is the number of fission products from a single fission of fissile nuclide i .

The variance of the previous sum satisfy :

$$\text{Var}\left(\sum_{k=1}^{N_{FP}} \gamma_{i,k}\right) = 0 \quad (10)$$

Then, the correlation $r_{i,j,k}$ between two fission yields $\gamma_{i,j}$ and $\gamma_{i,k}$ of the same fissile nuclide i is written as:

$$r_{i,j,k} = \frac{-\sum_{j=1}^{N_{FP}} \text{Var}(\gamma_{i,j})}{2 \sum_{j=1}^{N_{FP}-1} \sum_{k=j+1}^{N_{FP}} \sqrt{\text{Var}(\gamma_{i,j})\text{Var}(\gamma_{i,k})}} \quad (11)$$

A second option could be considered. It allows the use of a fission yields covariance data which was derived from the knowledge of isobaric chain yield found in the literature [13]. The formalism was first established by C. Devillers [11] and reported below. Diagonal terms (μ_{ii}) and off-diagonal terms (μ_{ij}) of the fission yields covariance matrix are respectively given by :

$$\mu_{ii} = \sigma_i^2 \left(1 - \frac{\sigma_i^2}{\sigma^2 + \sum_{j=1}^{N_A} \sigma_j^2}\right) \quad (12)$$

$$\mu_{ij} = -\frac{\sigma_i^2 \sigma_j^2}{\sigma^2 + \sum_{j=1}^{N_A} \sigma_j^2} \quad (13)$$

where σ^2 is the variance of the isobaric chain yield, σ_i^2 the variance of the independent fission yield γ_i and N_A the number of fission products in the same mass chain A . Noting $Y_C(A)$ the cumulative fission yield for mass chain A , this method satisfy both following constraints :

$$\sum_{k=1}^{N_{FP}} \gamma_{i,k} = \sum_{A=A_{min}}^{A_{max}} Y_C(A) = 2 \quad (14)$$

where A_{min} and A_{max} are respectively the minimal and the maximal mass number of fission products from the same fissile system.

The used mass chain uncertainties come from Rider (1993) database [13] which provides data for 60 fissile systems.

As described in section 2, DARWIN/PEPIN2 code uses the IncerD supervisor module to perform QOIs uncertainty quantification. Because of the sensitivity coefficients assessment, this task needs a large number of independent perturbed depletion runs (about 40 000 for a fuel cell depletion calculation) which are conducted in parallel mode using the OPENMPI/MPICH2 library.

5. Applications

Fission pulse and PWR-UO₂ fuel depletion was carried out to illustrate total decay heat uncertainty quantification with DARWIN/PEPIN2 code.

5.1. Fission pulse decay heat calculation

A fission of single atom of ^{235}U due to thermal neutron followed by a cooling period from 0 s up to 10^{13} s is considered ($^{235}\text{U}(T)$ - Thermal fission of ^{235}U). Decay heat of the resulting fission products and the associated uncertainties are calculated with DARWIN/PEPIN2 code using data from mainly JEFF-3.1.1 evaluation. In this case, there is no neutronic reaction but only radioactive decay process. Thus, nuclear data uncertainties which are propagated to decay heat come from :

- decay constant (λ),
- decay branching ratio (b),
- mean energy released by decay (E_{avg}),
- fission yield (γ) as initial concentration of Fission Products.

Based on the above correlation assumptions, nuclear data uncertainty propagation are performed and the results are summarized on figure 3. The used covariance matrix for independent fission yields is the one built from $Var(\sum_{k=1}^{N_{PF}} \gamma_{i,k}) = 0$. Through these graphs, we can notice that the major contributor on decay heat uncertainty is the fission yield followed by the mean decay energy. The other physical parameters as decay constants or decay branching ratios have smaller contribution on uncertainty decay heat.

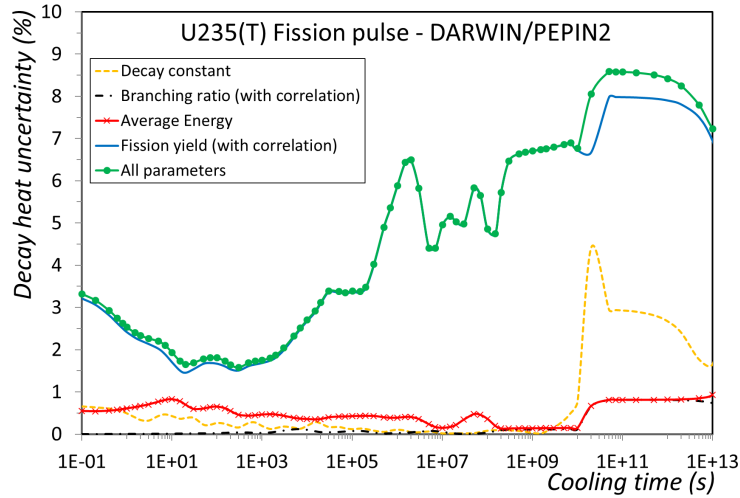


Figure 3: Decay heat uncertainty for $^{235}\text{U}(T)$ fission pulse using data from JEFF-3.1.1 library.

Both decay heat calculation results and the related uncertainties due to nuclear data from DARWIN/PEPIN2 code have been compared to experimental data (Akiyama [17]) and to Tobias statistical results as a compilation of several experiments [16].

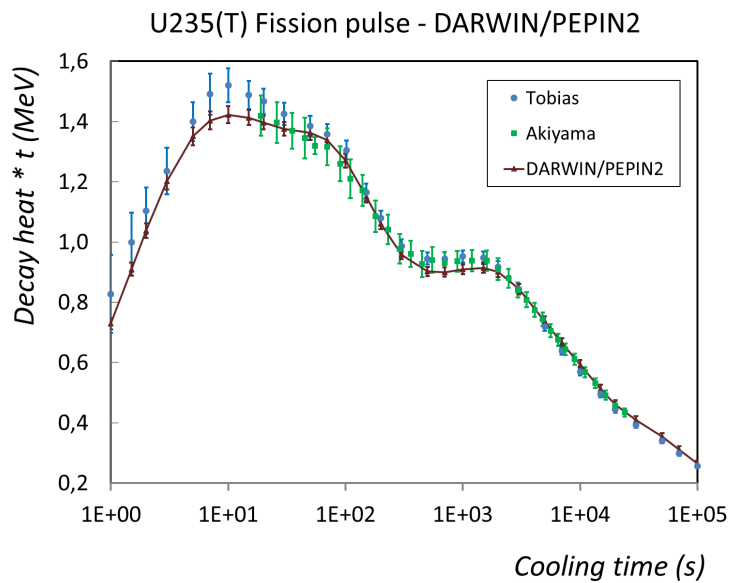


Figure 4: Decay heat uncertainties for $^{235}\text{U}(T)$ fission pulse using data from JEFF-3.1.1 library. Experiments versus calculations.

Results presented in figure 4 show a good agreement between calculation results and experimental data (Akiyama) while calculation results are under predicted compared to Tobias results. Nevertheless, calculation and Tobias error bars are consistent, that means, there is a common region covered by both error bars for each comparison point.

The large prevalence of fission yield in the observed decay heat uncertainties is subjected to discussion. As shown in figure 5, the use of the formalism established by C. Devillers, which take into account the two physical constraints defined by equation (14), shows a decrease of the fission yield contribution. But rather, if fission yield is assumed uncorrelated, an increase of this contribution is observed. These observations highlight that a considerable research work will have to be made to provide a reliable fission yield covariance data. For safety consideration in the decay heat uncertainty quantification, the fission yield covariance data built from equation (11) is retained as default option in DARWIN/PEPIN2 code.

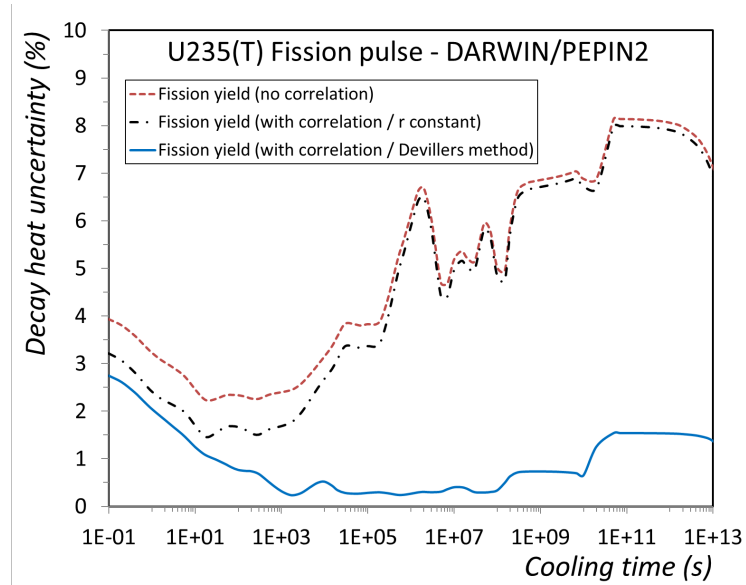


Figure 5: Contribution of fission yield uncertainty on decay heat uncertainty for $^{235}\text{U}(T)$ fission pulse using data from JEFF-3.1.1 library.

The first prominent peak of decay heat uncertainty (around 10^6s) seen in figures 3 and 5 is strongly due to the high uncertainty, from JEFF-3.1.1 library, of the independent thermal fission yield of ^{235}U producing ^{140}Xe . This independent fission yield and the associated uncertainty are respectively $0.3801 \times 10^{-1} \pm 0.5215 \times 10^{-2}$ (13.7%). ^{140}Xe radioactive disintegration leads to ^{140}La production which is the most contributor (42.7%) of the total decay heat at cooling time 10^6s . Figure 6 presents the activity uncertainty of ^{140}Xe ($T_{1/2} \approx 13.6\text{s}$) and ^{140}La ($T_{1/2} \approx 1.68\text{d}$).

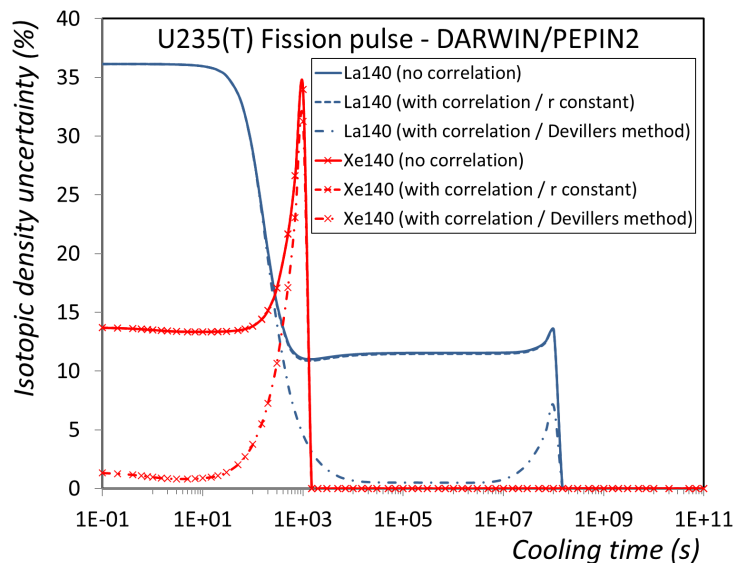


Figure 6: Contribution of fission yield uncertainty on ^{140}Xe and ^{140}La activity uncertainty for $^{235}\text{U}(T)$ fission pulse using data from JEFF-3.1.1 library.

In order to provide DARWIN/PEPIN2 code with the capability to use other international evaluations for decay heat uncertainty quantification, all relevant parameters uncertainties from ENDF/B.VII.1, JENDL/DDF-2015 & JENDL/FPY-2011 have been extracted and stored in specific DARWIN/PEPIN2 code input libraries. Then, decay heat uncertainty have been also calculated with the previous others international nuclear data. We emphasize hereafter some characteristics of each evaluation:

- The number of fissioning systems vary from one evaluation to another. JEFF-3.1.1 provides 39 fissioning systems while ENDF/B-VII.1 and JENDL/FPY-2011 provide respectively 61 and 60.
- Table 2 presents the distribution of ^{235}U thermal fission yield uncertainties as function of nuclide half-life for ENDF/B.VII.1, JENDL/FPY-2011 and JEFF-3.1.1 evaluations. We can emphasize that:
 - for JEFF-3.1.1: 68% of independent fission yield have their relative uncertainty value in the range 30% - 40%,
 - for ENDF/B-VII.1: 76% of independent fission yield have their relative uncertainty value in the range 50% - 70%,
 - for JENDL/FPY-2011: 78% of independent fission yield have their relative uncertainty value in the range 50% - 70%.

Half-life range (s) ⇒ Uncertainty range (%) ↓	0.0 - 10 ²			10 ² - 10 ⁴			10 ⁴ - 10 ⁷			10 ⁷ - 10 ¹⁰			10 ¹⁰ - 10 ³²			0.0 - 10 ³² (All non stable nuclides)		
	(1)	(2)	(3)	(1)	(2)	(3)	(1)	(2)	(3)	(1)	(2)	(3)	(1)	(2)	(3)	(1)	(2)	(3)
0.0 - 3.5	0	23	22	0	5	5	0	1	1	0	0	0	0	0	0	0	29	28
3.5 - 5.0	0	18	18	0	4	4	0	1	1	0	0	0	0	0	0	0	23	23
5.00 - 10.0	13	24	24	8	20	20	0	7	7	1	1	2	0	0	1	22	52	54
10.0 - 15.0	19	10	11	5	7	7	0	2	2	0	1	1	0	2	2	24	22	23
15.0 - 20.0	62	5	4	8	5	5	1	4	5	0	1	1	2	0	2	73	15	17
20.0 - 30.0	94	10	13	15	3	3	3	2	2	0	0	0	1	0	0	113	15	18
30.0 - 40.0	341	11	12	101	5	5	90	2	2	15	0	0	36	2	2	583	20	21
40.0 - 50.0	17	7	11	7	3	4	4	2	3	2	1	1	0	0	1	30	13	20
50.0 - 70.0	0	405	464	3	98	96	0	88	87	0	19	19	0	23	27	3	633	693
70.0 - 100.	0	0	52	0	0	6	0	0	1	0	0	2	0	0	1	0	0	0
> 100.0	0	0	0	0	0	0	0	0	0	0	0	0	0	0	0	0	0	0
Total	546	513	631	147	150	155	98	109	111	18	23	26	39	27	36	848	822	959

Table 2: Distribution of ²³⁵U thermal fission yield uncertainties with fission product half-life. JEFF3.1.1 (1), ENDF/B-VII.1 (2) and JENDL/FPY-2011 (3)

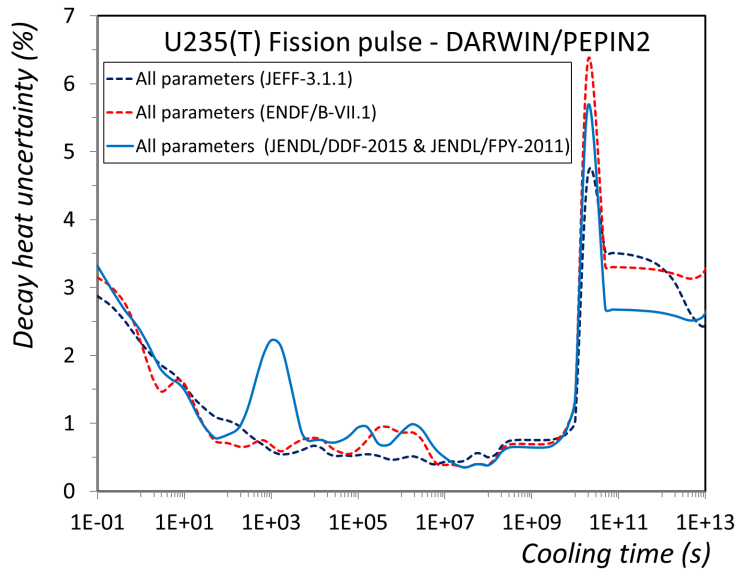


Figure 7: Contribution of all uncertainty physical parameters from JEFF-3.1.1, ENDF/B-VII.1 and JENDL/DDF-2015+JENDL/FPY-2011

Figure 7 presents the decay heat uncertainties due to nuclear data which have been computed by DARWIN/PEPIN2 using JEFF-3.1.1, ENDF/B-VII.1 and JENDL/DDF-2015+JENDL/FPY-2011. Only nuclear data uncertainties provided by these evaluations have been propagated and C. Devillers formalism was used to define the fission yield covariance data. Under this assumption, fission yields contribution on the decay heat uncertainty is shown in figure 8 while figures 9, 10 and 11 display respectively the mean energy, decay constant and decay branching ratio contributions. Whatever the evaluation, at short cooling times ($t_c < 10^2 s$), the decay heat uncertainty is dominated by fission yield contribution. At very short cooling times ($t_c < 1 s$), ENDF/B-VII.1 and JENDL/FPY-2011 give higher uncertainty than JEFF-3.1.1 as expected from table 2. Indeed, most

of highly uncertain fission yield match very short half-life fission products, ENDF/B-VII.1 and JENDL/FPY-2011 providing respectively 49% (405/822) and 48% (464/959) very short life fission products with fission yield relative uncertainty within [50% – 70%]. JEFF-3.1.1 provides 40% (341/848) short life fission products with fission yield relative uncertainty within [30% – 40%] and 2% (17/848) within [40%–50%]. At very long cooling times, beyond 10^{10} s, decay heat uncertainty is dominated by decay constant contribution for all evaluations (see figures 7 and 10), but this large relative uncertainty value is related to very small value of decay heat (see figure 3). Decay heat uncertainty curve from JENDL/DDF-2015 nuclear data displayed in figure 7 shows one prominent peak at cooling time around 10^3 s ($\sim 2.3\%$) which is due to decay energy contribution. One particular fission product is the main contributor to this peak, the ^{143}La which contributes around 4% to total decay heat at 10^3 s with high mean decay energy uncertainty (51.05%) in JENDL/DDF-2015 while the corresponding uncertainties are respectively 1.98% in ENDF/B-VII.1 and 0.78% in JEFF-3.1.1. A secondary peak ($\sim 1\%$) due to decay energy appears at 10^6 s for JENDL/DDF-2015 and ENDF/B-VII.1 decay heat uncertainty curves which are mainly caused by ^{140}La for JENDL/DDF-2015, the major contributor to decay heat ($\sim 42.7\%$), and ^{132}I for ENDF/B-VII.1 contributing to 15.5% of total decay heat. The relative uncertainty of ^{140}La mean decay energy is 1% for JENDL/DDF-2015 while it is respectively 0.54% and 0.26% for ENDF/B-VII.1 and JEFF3.1.1. The relative uncertainty of ^{132}I mean decay energy reaches 2.56% for ENDF/B-VII.1 while it stays minor (0.93%) for both JENDL/DDF-2015 and JEFF3.1.1. As figure 10 shows, decay constant contribution to decay heat uncertainty is small whatever the evaluation, except at very long time ($t_c > 10^{10}$ s) where decay heat have been considerably decreased and become meaningless.

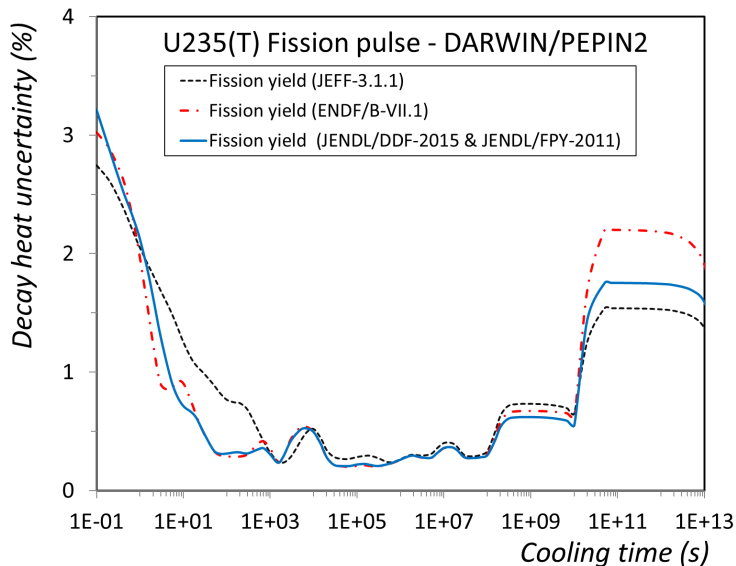


Figure 8: Contribution of fission yield uncertainty from JEFF-3.1.1, ENDF/B-VII.1 and JENDL/DDF-2015+JENDL/FPY-2011.

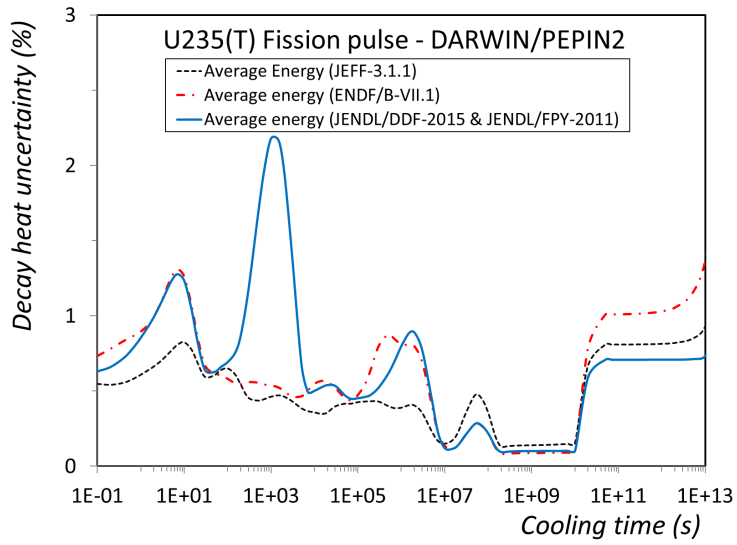


Figure 9: Contribution of mean decay energy uncertainty from JEFF-3.1.1, ENDF/B-VII.1 and JENDL/DDF-2015+JENDL/FPY-2011.

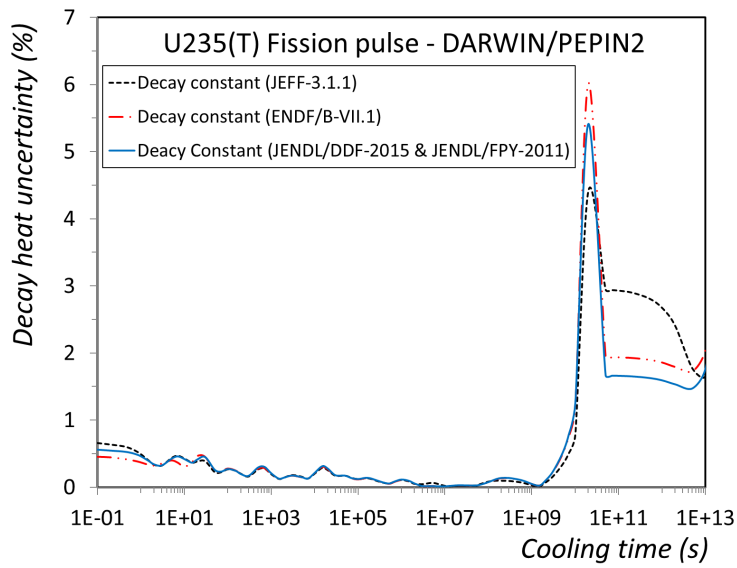


Figure 10: Contribution of decay constant uncertainty from JEFF-3.1.1, ENDF/B-VII.1 and JENDL/DDF-2015+JENDL/FPY-2011.

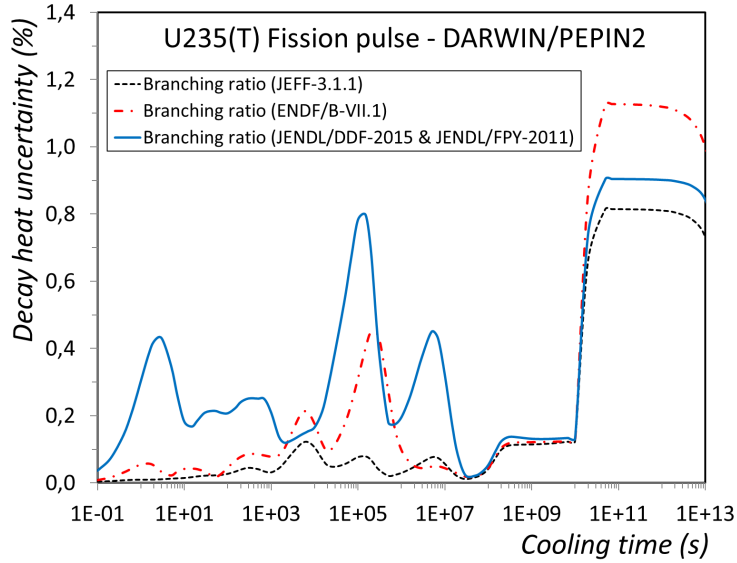


Figure 11: Contribution of decay branching ratio uncertainty from JEFF-3.1.1, ENDF/B-VII.1 and JENDL/DDF-2015+JENDL/FPY-2011.

Decay branching ratio contribution is insignificant for JEFF-3.1.1 (see figure 11) and, to lesser extent, for ENDF/B-VII.1. It reaches 0.8% at $t_c = 10^5 s$ for JENDL/DDF-2015. The following description is intended only to highlight the impact such a few inconsistencies have on both how dealing with and on the result. As an example, figure 13 shows that both this major peak and the first one which appears around 1s are mainly caused by the contribution of ^{97}Zr . Figure 12 presents decay pathways leading to ^{97}Zr from the very short life ^{98m}Y ($T_{1/2} \approx 2s$) fission product. The branching ratio value with the associated absolute uncertainty for each branch is reported. This figure shows differences between the three used evaluations. Unlike the two other evaluations, in JENDL/DDF-2015 description, ^{98m}Y have a third disintegration route producing ^{98}Y and this later nuclide decreases to ^{97}Zr . We emphasize that one of the three disintegration pathways from ^{98m}Y ($^{98m}\text{Y} \rightarrow ^{97}\text{Zr}$) have an absolute branching ratio uncertainty which differs from the two other ($0.01 \neq 0.1$).

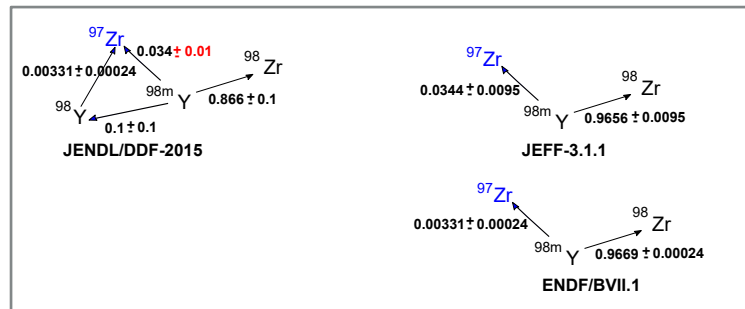


Figure 12: Decay pathways leading to ^{97}Zr from ^{98m}Y

As has been mentioned already in section 4.1, the default choice is to adopt 0.1 as the common value for each branching ratio uncertainty. This aimed to preserve the uncertainty value

of the major decay pathway but can lead to enhance the uncertainty value of minor decay pathways. It produces the red dashed curve in figure 12 as a result. The green dashed curve plotted in figure 13 corresponds to the choice of 0.01 as the common value for each branching ratio uncertainty and shows the disappearance of the two first peaks due to ^{97}Zr contribution.

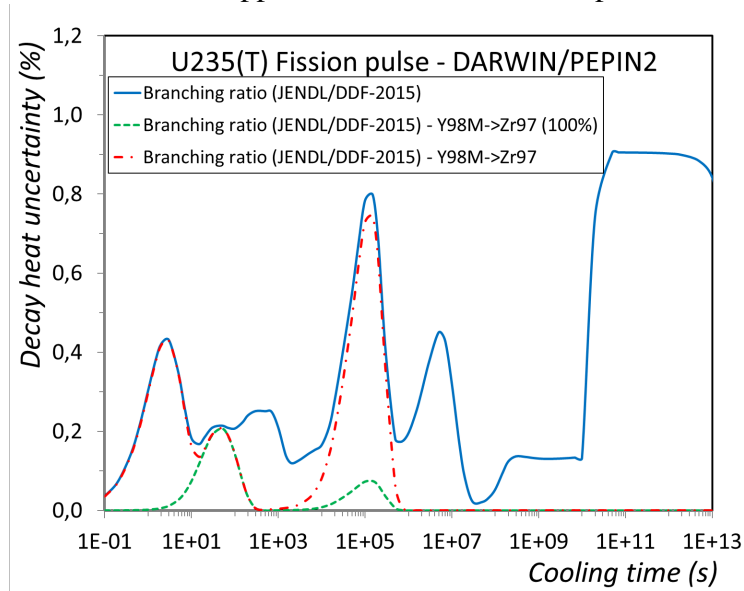


Figure 13: Contribution of decay branching ratio uncertainty from JEFF-3.1.1, ENDF/B-VII.1 and JENDL/DDF-2015+JENDL/FPY-2011.

Through this fission pulse illustrative study, final quantified decay heat uncertainties depend on the adopted assumptions to deal with both the lack of some nuclear covariance data provided by nuclear data evaluations and the few inconsistencies of nuclear data uncertainties. As an explicit example, many nuclide contributing to decay heat at short cooling times have no decay energy uncertainties provided by evaluations. To measure the impact of these unknown uncertainties, we did some calculations which assume that each unknown decay energy uncertainty shall be taken as the decay energy value, that is, the relative unknown decay energy uncertainty is fixed to 100%. Results are summarized in figure 14 which shows that whatever the evaluation, unknown decay energy uncertainties could have a strong influence on the quantified decay heat uncertainty at short cooling times, nevertheless limited to 10^3 s.

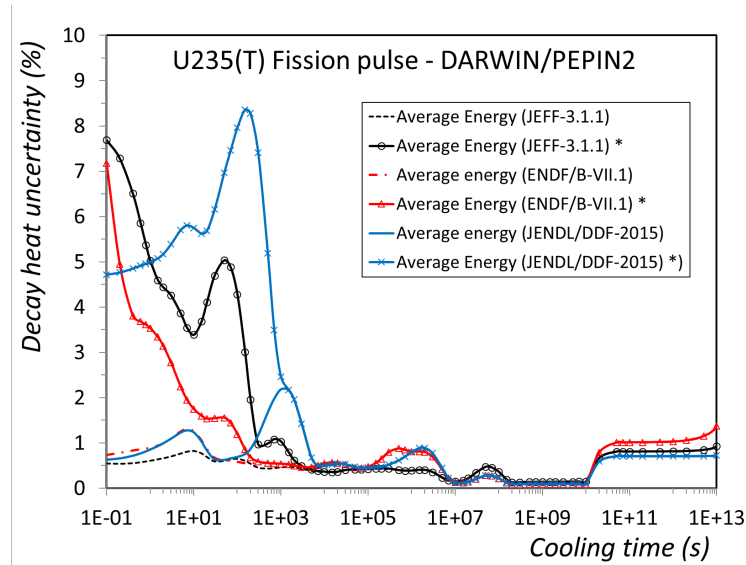


Figure 14: Impact of unknown decay energy uncertainties for JEFF-3.1.1, ENDF/B-VII.1 and JENDL/DDF-2015+JENDL/FPY-2011.

In this figure, curves which are captioned with asterisk (*) indicate that unknown relative decay energy uncertainty has been fixed to 100%.

5.2. Decay heat from PWR fuel cell calculation

A second application is discussed in this section and it concerns the total decay heat uncertainty quantification of PWR-UO₂ fuel depletion, that means the in-core fuel depletion is followed by cooling times after the reactor shutdown. As additional parameter governing the nuclide transmutation during the reactor operation, neutronic reaction cross section plays an important role to decay heat uncertainty quantification. To measure the impact of cross section uncertainties, we consider two distinctive assumptions according to DARWIN/PEPIN2 code capability:

- Decay heat sensitivity coefficients to cross section are computed by considering that cross section perturbations do not impact the neutron fluxes. Then, only one nominal transport calculation is performed with APOLLO2 code, providing nominal neutronic data (neutron fluxes, self-shielded cross sections, . . .) used in DARWIN/PEPIN2 depletion calculations.
- Decay heat sensitivity coefficients to cross section are computed by taking into account the neutron flux perturbation due to cross section perturbation. By this method, the direct perturbation calculations are applied for cross section parameters, one by one, during the neutron transport code step. Because of the computational cost attached to this configuration, we deal with only few major cross sections.

The entire results discussed in the following section come from the use of libraries based on JEFF-3.1.1 nuclear data evaluation.

5.2.1. Uncertainty quantification by assuming neutron fluxes are not affected by isotopic concentration perturbations

5.2.1.1. Calculation scheme.

An UO₂ fuel cell (4.1% wt ²³⁵U) calculation was performed with the APOLLO2.8 code, which aims to compute multi-group (the SHEM 281 group energy group structure) neutron flux spectra and self-shielded cross sections at well defined burnup steps from 0. MWd/tU to 46 050 MWd/tU. A configuration of infinite lattice, i.e a reflection condition as a boundary condition is considered. Neutron spectra and self-shielded cross sections are stored in specific database SAPHYB file. Once available from APOLLO2.8 calculation, the SAPHYB file is used as DARWIN/PEPIN2 code input to provide it the required multi-group self-shielded cross sections and neutron flux spectra for depletion calculation with the depletion chain (~2600 nuclides) dedicated to fuel cycle and radioactivity studies. The irradiation phase calculation, from 0 MWd/tU to 46 050 MWd/tU, is followed by cooling stage from 0 sec to 10¹³ sec. Decay heat physical quantity is requested as outputs during the cooling period. Supplementing this usual nominal calculation, IncerD module is carried out to perform decay heat sensitivity and uncertainty quantification by implementing the already described methodology. As has been mentioned in section 4, covariance matrices associated to neutron reaction cross sections come from COMAC-V2.0 database in 26 energy groups mesh. Depletion calculation is performed with a one group condensed microscopic neutron reaction rate from neutron spectra and microscopic cross sections in 281 energy groups structure expressed by:

$$\tau^r = \sum_{g=1}^{281} \tau_g^r = \sum_{g=1}^{281} \sigma_g^r \Phi_g, \quad (15)$$

with :

- σ_g^r the neutron microscopic cross section of a given nuclide for a given reaction type r in energy group g ;
- Φ_g the neutron flux in energy group g .

We remind that neutron fluxes are assumed not to be affected by microscopic cross sections perturbations. Two procedures have been implemented to compute sensitivity coefficients of decay heat to microscopic cross sections by direct perturbation method :

- The first method which is used as a standard way is based on the perturbation of the one group condensed microscopic reaction rate τ^r for each r -typ reaction. That means:

$$S_{DH/\tau^r} = \frac{DH(\tilde{\tau}^r) - DH(\tau^r)}{\tilde{\tau}^r - \tau^r} \times \frac{\tau^r}{DH(\tau^r)} \quad (16)$$

where :

$$\tilde{\tau}^r = \tau^r (1 + \alpha) \quad (17)$$

with : $\alpha \cdot \tau^r = \sqrt{\text{var}(\tau^r)} = \sqrt{{}^t S_{\tau^r/\sigma_{1G}} \cdot \text{cov}(\sigma_{1G}) \cdot S_{\tau^r/\sigma_{1G}}}$

The original multi-group cross sections covariance data from COMAC-V2.0 ($n_g = 26$ or $n_g = 33$) have to be condensed in one group (1G) using the following rule :

$$cov(\sigma_{1G}) = {}^t S_{\tau_{ng}^r} \cdot cov(\sigma_{ng}) \cdot S_{\tau_{ng}^r}$$

The sensitivity vector $S_{\tau_{ng}^r}$ is expressed by :

$$S_{\tau_{ng}^r} = \left[\frac{\partial \tau^r}{\partial \sigma_g^r} \times \frac{\sigma_g^r}{\tau^r} \right]_{1 \leq g \leq ng} = \left[\frac{\tau_g^r}{\tau^r} \right]_{1 \leq g \leq ng}$$

(Note that $\frac{\partial \tau^r}{\partial \sigma_g^r} = \frac{\sum_{g=1}^{ng} \sigma_g^r \Phi_g}{\partial \sigma_g^r} = \Phi_g$).

S_{DH/τ^r} and its transposed are combined with $cov(\sigma_{1G})$ to obtain decay heat uncertainty due to cross section covariance matrix propagation.

- The second method is optional and aims to compute multi-group (*MG*) sensitivity coefficients of decay heat to perturbation of each *r*-typ microscopic reaction rate within all COMAC energy groups mesh. For a given *r*-typ microscopic reaction rate, reaction rate value in each COMAC energy group mesh is perturbed one by one, before the condensation to one group is carried out. That means:

$$S_{DH/\tau^r}^g = \frac{DH(\tilde{\tau}^r) - DH(\tau^r)}{\tilde{\tau}^r - \tau^r} \times \frac{\tau^r}{DH(\tau^r)} \quad (18)$$

where :

$$\tilde{\tau}^r = \sum_{i \notin g} \tau_i^r + \sum_{i \in g} \tau_i^r (1 + \alpha_g)$$

with : $\alpha_g \cdot \sum_{i \in g} \tau_i^r = \sqrt{var(\tau_g^r)}$

S_{DH/τ^r}^g and its transposed are combined with $cov(\sigma_{ng})$ to obtain the decay heat uncertainty due to cross section covariance matrix propagation.

For both methods, when the perturbation concerns the fission cross section or the radiative capture cross section, the total cross section is changed in compliance with the introduced perturbation.

5.2.1.2. Results.

Decay heat uncertainties due to (n, γ), (n,*f*), (n,2*n*) of ²³⁵U, (n, γ), (n,*f*), (n,2*n*) of ²³⁸U and (n, γ), (n,*f*), (n,2*n*) of ²³⁹Pu which was carried by both one group sensitivity coefficient procedure (1G-procedure) and multi-group sensitivity coefficient procedure (MG-procedure) above are plotted (Figure 15). There are no significant differences between the results provided by the two procedures.

At short cooling times up to about 10⁵ s, the decay heat uncertainty due to ²³⁸U cross-sections uncertainties is about three times greater than that due to ²³⁵U or ²³⁹Pu cross sections uncertainties. This is due to the fact that ²³⁹U (β^- -decay) and ²³⁹Np (β^- -decay and γ decay) contributions to total

decay heat are among the most dominant contribution at short cooling times, and that the formation of these two radionuclides come entirely from the neutron capture by ^{238}U . The contribution of ^{239}Pu , fed by the decay paths $^{239}\text{U}(\beta^-)^{239}\text{Np}$ and $^{239}\text{Np}(\beta^-)^{239}\text{Pu}$, is important at long cooling time (between 10^{10} s and 10^{12} s), and the most important at 10^{12} s .

The MG-procedure aims to get more detailed sensitivity analysis like sensitivity at the energy group level. When applied to decay heat uncertainty quantification, the associated calculation cost is higher than that corresponding to 1G-procedure. This later was chosen as the default option for cross section uncertainty propagation.

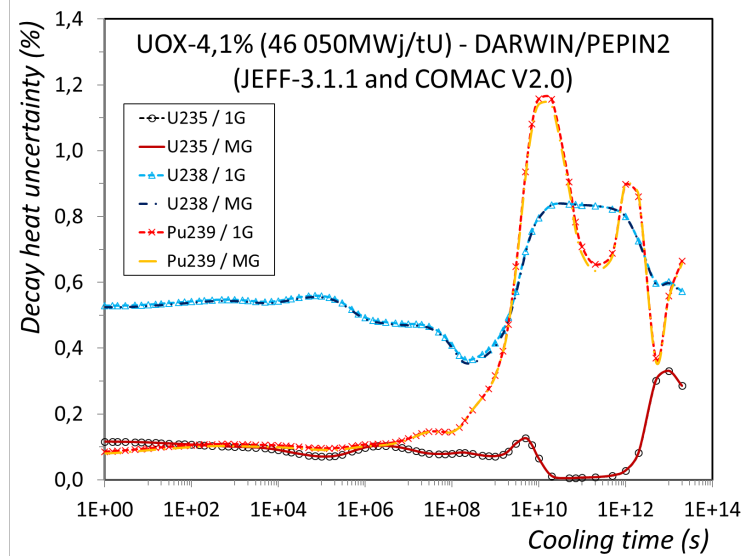


Figure 15: One group cross section perturbation compared to multigroup cross section perturbation for irradiated nuclear fuel UOX 4.1% at 46 050 MWj/tU (JEFF-3.1.1 library).

Figure 16 provides the total decay heat uncertainty as function of cooling time and details the part of this uncertainty due to each type of nuclear data.

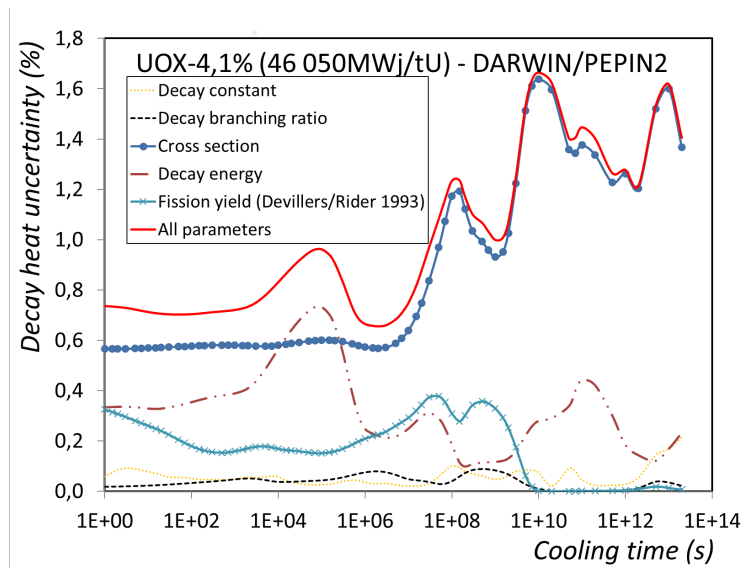


Figure 16: Contribution of all parameters on Decay heat uncertainty for irradiated nuclear fuel UOX 4.1% at 46 050 MWj/tU (JEFF-3.1.1 library).

The fission yield correlation hypothesis adopted here is th C. Devillers method to minimize the contributions of yield uncertainties. Under this assumption, the uncertainties attached to cross sections followed by those of decay energies are, respectively, the first and the second contributor to the uncertainty of the total decay heat observed, mainly at short cooling times.

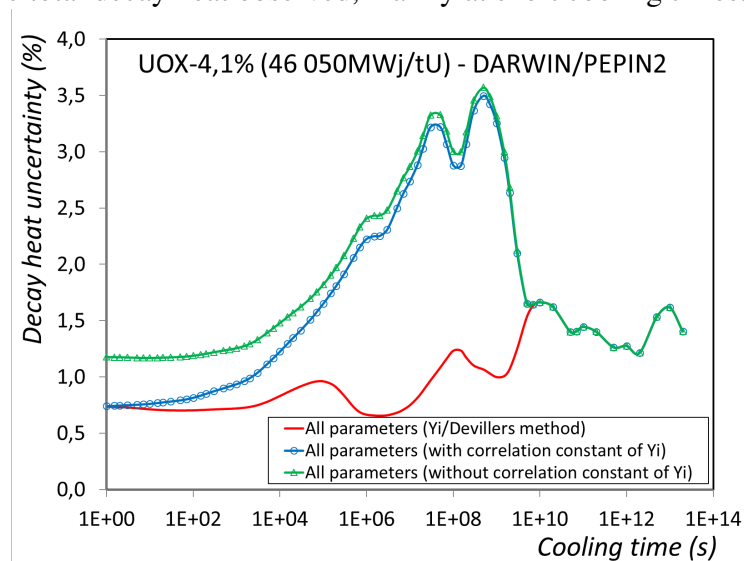


Figure 17: Total decay heat uncertainty for irradiated nuclear fuel UOX 4.1% at 46 050 MWj/tU (JEFF-3.1.1 library) function of fission yield correlation hypothesis.

As shown in figure 17, it is important to note that the level of total decay heat uncertainty is highly dependent on the correlation hypothesis adopted for fission yields. The most conservative hypothesis is the absence of correlation of fission yields, followed closely by the correlation hypothesis induced by fixing the sum of these yields to constant. Taking into account additional

physical constraints that correspond to the hypothesis adopted in C. Devillers method leads to a sharp decrease in the contribution of fission yield uncertainties to the total decay heat uncertainty.

5.2.2. Uncertainty propagation where neutron fluxes are affected by isotopic concentration perturbations

The objective of the following illustrative calculation is to expose, through a few effective cross sections identified as influential, the implemented approach to take into account the feedback of isotopic concentration perturbations, due to cross section perturbation, and the neutron fluxes, when quantifying the total decay heat uncertainty. Results are compared to those from the previous assumption which considers that isotopic concentration perturbations do not affect the neutron fluxes.

5.2.2.1. Calculation scheme.

Unlike the previous calculation, the sensitivity coefficients of cross-section are evaluated using one nominal SAPHYB file which was established under nominal calculation state and a set of perturbed SAPHYB files (one file for one perturbed reaction) which store perturbed cross-section and resulting neutron flux values. Each perturbed SAPHYB comes from a neutron transport calculation by perturbing one isotopic reaction type multi-group cross-section. A self-shielding calculation is realized at the beginning of the cycle before a specific module named CHABINT in APOLLO2 code is used to introduce the desired perturbation rate in the isotopic reaction type self-shielded cross-section of interest. Then neutron flux followed by the atom density calculations are performed.

We consider here six major nuclide with the following ten neutron reactions :

- $^{235}\text{U}(n, \gamma), ^{235}\text{U}(n, f),$
- $^{238}\text{U}(n, \gamma), ^{238}\text{U}(n, f),$
- $^{239}\text{Pu}(n, \gamma), ^{239}\text{Pu}(n, f),$
- $^{240}\text{Pu}(n, \gamma)$
- $^{241}\text{Pu}(n, \gamma), ^{241}\text{Pu}(n, f),$
- $^{242}\text{Pu}(n, \gamma)$

Absorption and total cross section are changed in compliance with the introduced perturbation when the fission cross section or the radiative capture cross section is perturbed.

5.2.2.2. Results.

Figure 18 shows a comparison of the total decay heat uncertainties provided by the two propagation calculation contexts, with feedback (with FB) and without feedback (without FB). It supplies also the decay heat uncertainties due to cross section. Up to 10^8 s, the decay heat uncertainty

obtained when taking into account the feedback between isotopic concentration and neutron fluxes is lower than that obtained with non-retroaction hypothesis. It can be explained by the observed difference between cross section uncertainties contributions.

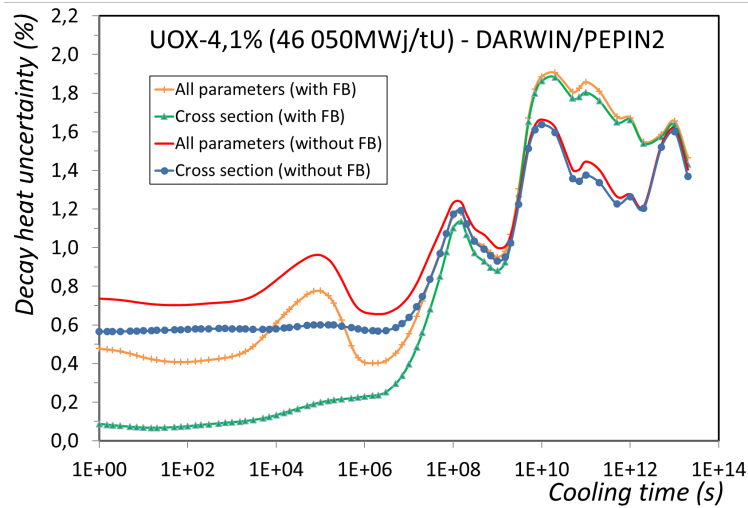


Figure 18: Multigroup cross section perturbation by transport code APOLLO2 (FB) versus mono-kinetic cross section perturbation by depletion code DARWIN/PEPIN2 (without FB) - UOX 4.1% at 46 050 MWj/tU.

As shown by figures 19, 20, 21, 22, up to 10^8 s, among the ten considered microscopic neutron reaction rate, the most difference in decay heat sensitivity results between the two studied hypothesis is for $^{238}\text{U}(n, \gamma)$. This is due to the fact that ^{239}U and ^{239}Np , produced by $^{238}\text{U}(n, \gamma)$, are dominant contributors to decay heat at these short cooling times. Pathway leading to these dominant contributors during the reactor operation and their respective relative contribution to total decay heat ($\%DH_{tot}$) are provided in table 3. ^{239}U and ^{239}Np concentrations are both less sensitive to $^{238}\text{U}(n, \gamma)$ when considering the feedback between isotopic concentration and neutron flux as indicate sensitivity coefficients provided in table 3.

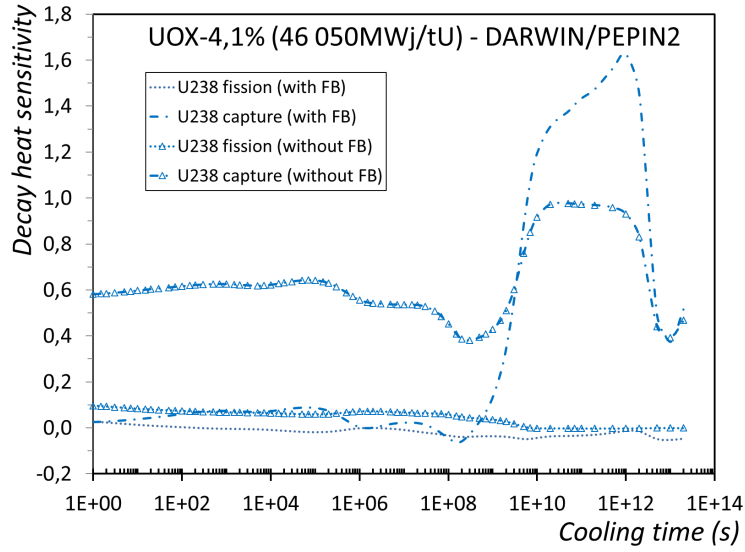


Figure 19: Cross section sensitivities of ^{238}U (UOX 4.1% at 46 050 MWj/tU) in the two cases without and with feedback (FB).

$t_{cooling}(s)$	^{239}U ($T_{1/2} = 23.5mn$)	^{239}Np ($T_{1/2} = 2.35d$)
1.0	2.9% DH_{tot}	2.8% DH_{tot}
10^2	5.0% DH_{tot}	5.1% DH_{tot}
10^5	-	20.1% DH_{tot}

Pathway : $^{238}\text{U}(n, \gamma) \rightarrow ^{239}\text{U}(\beta^-)^{239}\text{Np}$		
Relative sensitivity coefficient to $^{238}\text{U}(n, \gamma)$ of ^{239}U and ^{239}Np concentrations. $t_{cooling} \leq 10^5 s$		
	^{239}U	^{239}Np
with FB	0.51	0.52
without FB	0.97	0.97

Table 3: Some characteristics at different short cooling times

For long cooling times, after disappearance of most fission products by radioactive disintegration, major contributors to decay heat are long life nuclides, that means ^{241}Am (72.0% DH_{tot} - $T_{1/2} = 432.8y$) at $10^{10}s$, ^{240}Pu (52.0% DH_{tot} - $T_{1/2} = 6563y$) at $10^{11}s$ and ^{239}Pu (79.5% DH_{tot} - $T_{1/2} = 2.41 \times 10^4y$) at $10^{12}s$. During the operation of the reactor, pathway leading to these nuclides comes from $^{238}\text{U}(n, \gamma)$. As shown in table 4, their concentration become more sensitive to $^{238}\text{U}(n, \gamma)$ in the case of feedback between isotopic concentration and neutron flux, and therefore the total decay heat shown in figure 19.

$t_{cooling}(s)$	^{241}Am ($T_{1/2} = 432.8y$)	^{240}Pu ($T_{1/2} = 6563y$)	^{239}Pu ($T_{1/2} = 2.41 \times 10^4y$)
10^{10}	72% DH_{tot}	11% DH_{tot}	6.7% DH_{tot}
10^{11}	4.6% DH_{tot}	52.0% DH_{tot}	38.5% DH_{tot}
10^{12}	-	-	79.5% DH_{tot}

Pathway : $^{238}\text{U}(n, \gamma) \rightarrow ^{239}\text{U}(\beta^-) \rightarrow ^{239}\text{Np}(\beta^-) \rightarrow ^{239}\text{Pu}$ $(n, \gamma) \rightarrow ^{240}\text{Pu}(n, \gamma) \rightarrow ^{241}\text{Pu}(\beta^-) \rightarrow ^{241}\text{Am}$		
---	--	--

Relative sensitivity coefficient to $^{238}\text{U}(n, \gamma)$ of ^{241}Am , ^{240}Pu and ^{239}Pu concentrations			
	^{241}Am	^{240}Pu	^{239}Pu
$t_{cooling} = 10^{10} s$			
with FB	1.29	1.23	1.92
without FB	0.98	0.98	0.97
$t_{cooling} = 10^{11} s$			
with FB	1.27	1.23	1.90
without FB	0.98	0.98	0.97
$t_{cooling} = 10^{12} s$			
with FB	-	-	1.84
without FB	-	-	0.97

Table 4: Some characteristics at different long cooling times

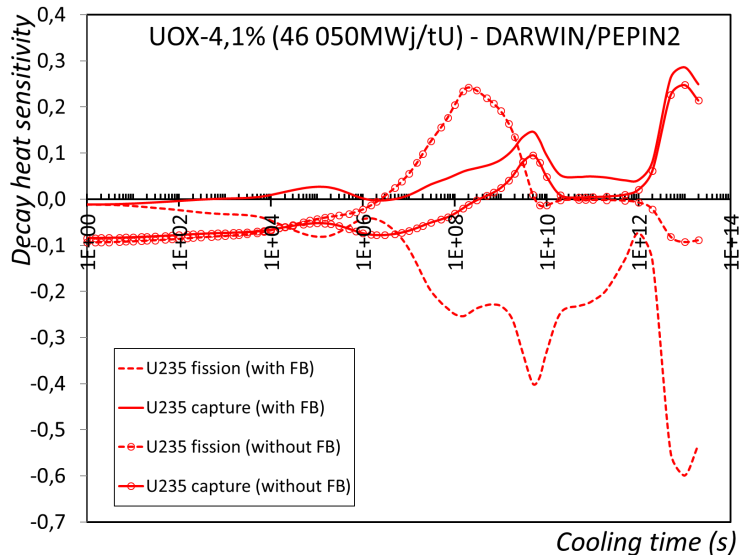


Figure 20: Cross section sensitivities of ^{235}U (UOX 4.1% at 46 050 MWj/tU) in the two cases without and with feedback (FB).

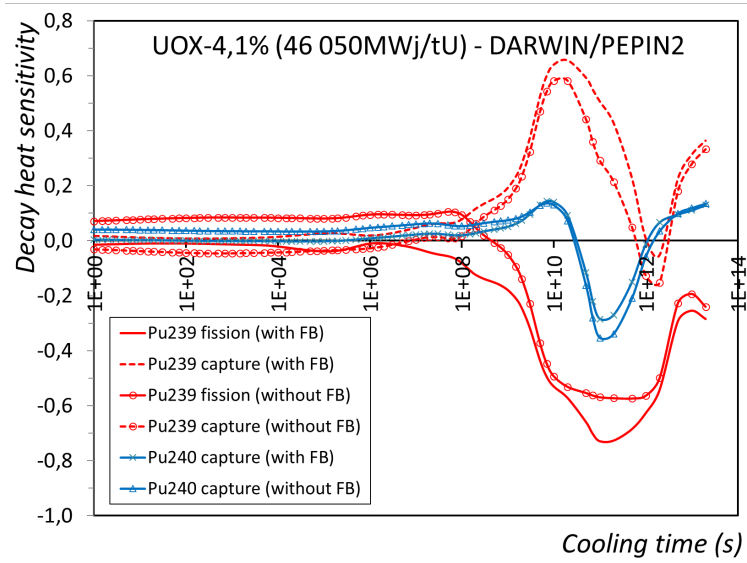


Figure 21: Cross section sensitivities of ^{239}Pu and ^{240}Pu (UOX 4.1% at 46 050 MWj/tU) in the two cases without and with feedback (FB).

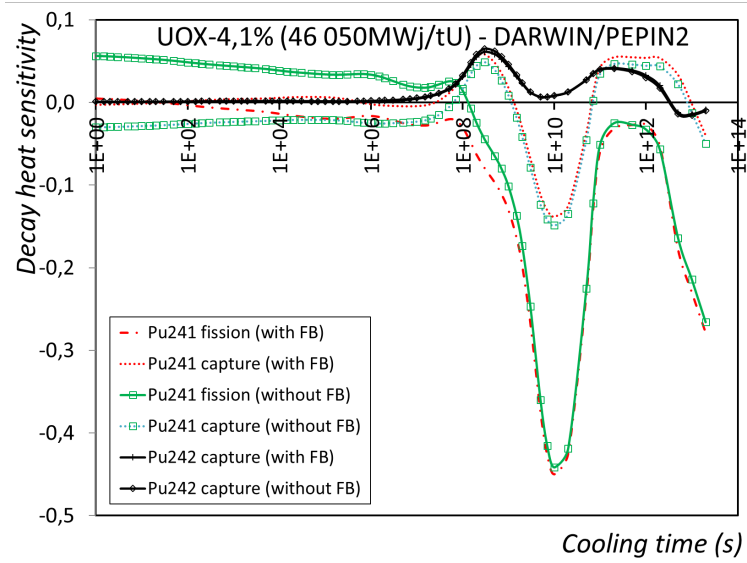


Figure 22: Cross section sensitivities of ^{241}Pu and ^{242}Pu (UOX 4.1% at 46 050 MWj/tU) in the two cases without and with feedback (FB).

6. Conclusion

We exposed through this paper the DARWIN/PEPIN2 inventory code capabilities in the field of nuclear data uncertainties propagation to physical quantity of interest as decay heat or atom density. References [24], [25] provide more validation and verification results of the exposed capabilities. This code is a powerful tool for helping engineers to implement a methodology of nuclear data uncertainties propagation which is best suited to their specific applications. For each time range of interest in safety or design studies related to spent fuel management (accidental situation, spent fuel transport, storage, etc. . .), maximum value of decay heat uncertainty due to the propagation of input nuclear data uncertainties is usually combined with other sources of uncertainty to get the total decay heat uncertainty. DARWIN/PEPIN2 code is a part of the DARWIN package [23] which is commonly used by French nuclear actors.

In order to gain confidence in the results of nuclear data uncertainties methodology propagation, it is of particular importance that calculation codes have the benefit of consistent and reliable data from evaluations. This is all the more important as the data are part of main contributors to the required response.

7. Acknowledgment

The authors are very grateful to EDF for its financial support in DARWIN/PEPIN2 code development.

They would also like to thank their colleagues Pierre Bellier and Sébastien Lahaye, respectively for the valuable guidance and expertise during the realization of the APOLLO2 calculations and for the helpful discussions.

Finally, they would especially like to thank Dr Cheikh Diop for his proofreading of this paper.

References

- [1] A. Tsilanizara, C.M. Diop, B. Nimal, M. Detoc, L. Lunéville, M. Chiron, T.D. Huynh, I. Brésard, M. Eid, J.C. Klein, B. Roque, P. Marimbeau, C. Garzenne, J.M. Parize & C. Vergne, "DARWIN: An Evolution Code System for a Large Range of Applications", *Journal of Nuclear Science and Technology*, Supplement 1, 845-849 (March 2000).
- [2] E. Brun, F. Damian, C.M. Diop, E. Dumonteil, F.X. Hugot, C. Jouanne, Y.K. Lee, F. Malvagi, A. Mazzolo, O. Petit, J.C. Trama, T. Visonneau, A. Zoia, "TRIPOLI-4®, CEA, EDF and AREVA reference Monte Carlo code", *Annals of Nuclear Energy* 82, 151-160 (2015).
- [3] M.A. Kellett, O. Bersillon and R.W. Mills, "The JEFF-3.1/-3.1.1 Radioactive Decay Data and Fission Yields Sub-libraries", *JEFF Report* 20, (2009).
- [4] C.J. Werner, J.S. Bull, C.J. Solomon, et al., "MCNP6.2 Release Notes", LA-UR-18-20808, (2018).
- [5] M.B. Chadwick, P. Oblozinsky, M. Herman *et al.*, "ENDF/B-VII.1 nuclear data for science and technology: Cross sections, covariances, fission product yields and decay data", *Nuclear Data Sheets* Vol 112, Issue 12, 2887-3152 (2011).
- [6] G. Rimpault et al., "The ERANOS Code and Data System for Fast Reactor Neutronic Analyses", *Proc. Int. Conf. PHYSOR 2002*, Seoul, Korea, October 7-10, 2002
- [7] P. Filliatre, L. Oriol, C. Jammes, L. Vermeeren, "Reasons why Plutonium 242 is the best fission chamber deposit to monitor the fast component of a high neutron flux", *Nuclear Instruments and Methods in Physics Research*, A 593, 510-518, 2008
- [8] J. Katakura, "JENDL FP Decay Data File 2011 and Fission Yields Data File 2011", *Nuclear Data Center JAEA-Data/Code* 2011-025, (2012).
- [9] M. Fadil, B. Rannou, et al., "About the production rates and the activation of the uranium carbide target for SPIRAL 2", *Nuclear Instruments and Methods in Physics Research*, B 266, 4318-4321, 2008
- [10] J. Katakura and F. Minato, "JENDL Decay Data File 2015", *Nuclear Data Center JAEA-Data/Code* 2015-030, (2016).
- [11] C. Devillers, "The Importance of Fission Product Nuclear Data in Reactor Design and Operation", *IAEA-213*, Vol 1, p 61-91, (1977).
- [12] P. Archier, C. de Saint-Jean et al., "COMAC: nuclear data covariance matrices library for reactor applications", *PHYSOR 2014*, Kyoto, JAPAN, (2014).
- [13] T. R. England and B. F. Rider, "Evaluation and Compilation of Fission Product Yields 1993", *Tech. Rep.*, LA-UR-94-3106, ENDF-349, (1994).
- [14] R. Sanchez, I. Zmijarevic, M. Coste-Delclaux, E. Masiello, S. Santandrea, E. Martinolli, L. Villate, N. Schwartz & N. Guler, "APOLLO2 YEAR 2010", *Nuclear Engineering and Technology*, Vol. 42, No. 5, (October 2010).
- [15] <https://root.cern.ch/>
- [16] A. Tobias, "Derivation of Deacya Heat Benchmark for U235 and PU239 by a Least Squares Fit to Measured Data", *CEGB report* RD/B/6210/R89, (1989)
- [17] M. Akiyama, "An S. Measurements of fission product decay heat for fast reactor", *Proceedings of International Conference on Nuclear Data for Science and Technology*, (1982), Antwerp, Belgium, September 6-10
- [18] J. Katakura, "JENDL FP Decay Data File 2011 and Fission Yields Data File 2011", *JAEA-Data/Code* 2011-025 (Mar. 2012).
- [19] J. Katakura, F. Minato, K. Ohgama, "Revision of the JENDL FP Fission Yield Data", *EPJ Web of Conferences* 111, 08004 (Mar. 2016).
- [20] Futoshi Minato, "JENDL/FPY-2011(corrected version)", *Nuclear Data Center at JAEA*, Document A (Apr. 2017).
- [21] J. Rebah, "Incertitudes sur la Puissance Résiduelle dues aux incertitudes sur les données de Produits de Fission", *Thesis*, 1998
- [22] V. Vallet, S. Lahaye, A. Tsilanizara, L. San Felice, R. Eschbach, "Deterministic Approach of the Decay Heat Uncertainty due to JEFF-3.1.1 nuclear data uncertainties with the CYRUS tool and the DARWIN2.3 Depletion Code", *PHYSOR 2014*, Kyoto, JAPAN, (2014).
- [23] J. Huyghe, V. Vallet, D. Lecarpentier, C. Reynard-Carette, C. Vaglio-Gaudard, "How to obtain an enhanced ex-

- tended uncertainty associated with decay heat calculations of industrial PWRs using the DARWN2.3 package", EPJ Nuclear Sci. Technol. 5, 8 (2019).
- [24] S. Lahaye, T.D. Huynh, A. Tsilanizara, "Comparison of deterministic and stochastic approaches for isotopic concentration and decay heat uncertainty quantification on elementary fission pulse", EPJ Web of Conferences 111, 09002 (2016)
- [25] S. Lahaye, T.D. Huynh, A. Tsilanizara, J.C. Jaboulay, S. Bourganel, "Comparisons between a priori Uncertainty Quantification and Calculation/Measurement Discrepancies Applied to the MERCI UO₂ Fuel Rod decay Heat Experiment", Transactions of the American Nuclear Society, Vol. 115, Las Vegas, NV, November 6-10, 2016